Linköping University Postprint

Numerical investigation of the validity of the Slater-Janak transition-state model in metallic systems

C. Göransson, W. Olovsson and I. A. Abrikosov

N.B.: When citing this work, cite the original article.

Numerical investigation of the validity of the Slater-Janak transition-state model in metallic systems

C. Göransson,[1] W. Olovsson,[2] and I. A. Abrikosov[1]

[1]*Department of Physics, Chemistry and Biology (IFM), Linköping University, SE-581 83 Linköping, Sweden*
[2]*Condensed Matter Theory Group, Department of Physics, Uppsala University, SE-751 21 Uppsala, Sweden*
(Received 20 May 2005; revised manuscript received 24 August 2005; published 19 October 2005)

According to the so-called Janak's theorem, the eigenstates of the Kohn-Sham Hamiltonian are given by the derivative of the total energy with respect to the occupation numbers of the corresponding one-electron states. The linear dependence of the Kohn-Sham eigenvalues on the occupation numbers is often assumed in order to use the Janak's theorem in applications, for instance, in calculations of the core-level shifts in materials by means of the Slater-Janak transition state model. In this work first-principles density-functional theory calculations using noninteger occupation numbers for different core states in 24 different random alloy systems were carried out in order to verify the assumptions of linearity. It is found that, to a first approximation, the Kohn-Sham eigenvalues show a linear behavior as a function of the occupation numbers. However, it is also found that deviations from linearity have observable effects on the core-level shifts for some systems. A way to reduce the error with minimal increase of computational efforts is suggested.

PACS number(s): 71.15−m, 71.23−k

I. INTRODUCTION

In density-functional theory[1,2] (DFT), a many-body system is described by noninteracting particles which have the same electron-density as the true many-body system. The ground-state electron-density minimizes the total-energy functional

$$E[n] = T_s[n] + \int dr n(r)[V_{\text{ext}}(r) + V_H(r)] + E_{\text{xc}}[n], \quad (1)$$

where $T_s[n]$ is the kinetic energy for noninteracting particles, V_{ext} the external potential of the system under consideration, V_H is the Coulomb potential, and $E_{\text{xc}}[n]$ the exchange-correlation energy. In DFT, all manybody interactions are contained within this last term, which usually is very amenable to approximations.[3]

Minimization of Eq. (1) yields a Schrödinger-like equation

$$[-\nabla^2 + V_{\text{ext}}(r) + V_H(r) + v_{\text{xc}}(r)]\psi_i = \varepsilon_i \psi_i, \quad (2)$$

where $v_{\text{xc}} = \delta E_{\text{xc}} / \delta n(r)$ is the exchange-correlation potential and ε_i the Kohn-Sham eigenvalue for the ith electron state. The electron-density for an N-electron system is given by

$$n(r) = \sum_{i=1}^{N} |\psi_i(r)|^2, \quad (3)$$

where the summation is taken over the N lowest one-electron states in Eq. (2). Equations (2) and (3) have to be solved self-consistently. Once self-consistency has been reached, the result is inserted into Eq. (1). Since in the DFT the real manybody problem is mapped onto the problem for noninteracting particles, the Kohn-Sham eigenvalues do not necessarily have physical meaning, though they describe the correct electron density.[4]

In a well-known paper, Janak[5] introduced an extension of the standard DFT, which made use of fractional occupation numbers for the electrons. Within this theory it is possible to show that the derivative of the total-energy functional with respect to an occupation number equals the corresponding Kohn-Sham eigenvalue, which is known as "Janak's theorem." After the publication of this theorem, its validity has been discussed.[6] Though being an interesting and important discussion, we do not comment on it in the present work. Despite the abovementioned discussion, Janak's theorem provided a new method to calculate the binding energy for electrons. Calculations for different occupation numbers for some systems have been performed in Refs. 7 and 8. The most widely used version of this method is the so-called "Slater-Janak transition state," which states that the binding energy equals the Kohn-Sham eigenvalue for a half-occupied state. This model is based on the assumption that the Kohn-Sham eigenvalues are *linear* functions of the occupation number. Though widely applied, this assumption behind the Slater-Janak transition state model, have not, to the best of our knowledge, been tested systematically.

Here we present DFT calculations investigating numerically the validity of the Slater-Janak transition state approach for 24 alloy systems. The paper is organized as follows. In Sec. II A we present the background of the Slater-Janak transition state picture and similar schemes, in Sec. II B we discuss the core-level shifts as an application of the theory and as a method to verify the assumption of linearity. The results are presented and discussed in Sec. III and the work is summarized in Sec. IV.

II. METHODOLOGY

A. Theory

In Ref. 5, Janak redefined the DFT charge density to be

$$n(\mathbf{r}) = \sum_i \eta_i |\psi_i(\mathbf{r})|^2, \qquad (4)$$

where the η_i is an occupation number for the state i $(0 < \eta < 1)$. Self-consistent solutions to Eqs. (2) and (4) can be found for a given set of η_i's, including sets containing noninteger occupation numbers.

By defining

$$\widetilde{T}_s = \sum_i \eta_i t_i,$$

where $t_i = \int d\mathbf{r} \psi_i^*(-\nabla^2)\psi_i$, one can construct a new, slightly different total-energy functional $\widetilde{E}$:

$$\widetilde{E} = \widetilde{T}_s + \int d\mathbf{r} n(\mathbf{r})[V_{\text{ext}}(\mathbf{r}) + V_H(\mathbf{r})] + E_{\text{xc}}[n]. \qquad (5)$$

Generally $\widetilde{E} \neq E$, but if the η_i's have the form of Fermi-Dirac distribution, $\widetilde{E}$ will be equal to E.

Using the above definition, it is possible to derive the so-called "Janak theorem"[5]

$$\frac{\partial \widetilde{E}}{\partial \eta_i} = \varepsilon_i. \qquad (6)$$

By integration of Eq. (6) one can connect the energies of the ground states of an N and an $(N+1)$ particle system

$$E_{N+1} - E_N = \int_0^1 \varepsilon(\eta_i) d\eta_i. \qquad (7)$$

Equation (7) can be used to calculate the change in total energy when removing one electron from the core, which will then be the core-level binding energy for that electron state, i.e., $E_{B_i} = \int_0^1 \varepsilon(\eta_i) d\eta_i$. It should be mentioned that Janak's theorem is only applicable to the highest occupied electron state.[3,5] However, the theorem has been used with success for core states.[9–11]

If the Kohn-Sham eigenvalue ε is a linear function of the occupation number η, the core-level binding energy can easily be calculated as

$$E_{B_i} = \int_0^1 \varepsilon_i(\eta_i) d\eta_i \approx \varepsilon_i(1/2) \qquad (8)$$

$$\approx \varepsilon_i(1) + \frac{1}{2}[\varepsilon_i(0) - \varepsilon_i(1)], \qquad (9)$$

where the evaluation at midpoint, Eq. (8), is the abovementioned Slater-Janak transition state.[5,12] Equation (9) is physically more transparent than Eq. (8), since it shows the separation of inital- and final-state effects (the first and second term, respectively) of the binding energy. Systems containing fractional occupation numbers do not necessarily represent any physical system,[8] but here the use of fractional occupation numbers is merely a way to numerically solve the integral, Eq. (7). Since the above method rests upon the assumption of linearity, it is important to verify its validity. In the present work we evaluate the linearity of the Kohn-Sham eigenvalues as a function of η and investigate if possible

deviations from linearity have any effect of physical observable.

B. Core-level shifts in alloys

The electronic states in a pure metal have a certain spectrum specific to the atomic species and the structure of the crystal. This spectrum will, in general, be different from the spectrum of the same atomic species in an alloy. This gives rise to the so-called core-level shifts (CLS), which is the difference in binding energy for the same electronic state between the alloy and the pure metal. The CLS can be divided into inital- and final-state contributions. The initial-state contribution is the shift in core-electron eigenstates and the final-state contribution is due to core-hole relaxation effects when removing the core electron.[13]

The transition-state (TS) model for calculating the CLS is one of the applications of Janak's theorem and the Slater-Janak transition state. Therefore, it provides a more physical approach to investigate the linearity of the Kohn-Sham eigenvalues. Usually, in theoretical calculations one employs either Eq. (8) and (9). It is worth to notice that the first of these two equations only requires two calculations, one for the reference system and one for the system in interest, in order to obtain the binding energy shift, whereas the latter requires two calculations per reference and studied systems, respectively, i.e., totally four calculations.

Though no meaningful absolute reference level for the lineup of one-electron eigenenergies exist,[14] the CLS are often related to the Fermi level, since this is convenient for metallic systems.[15] In our notation, this means that

$$\varepsilon_i(\eta_i) = E_F(\eta_i) - \varepsilon_i^{\text{OE}}(\eta_i),$$

where E_F is the Fermi-energy and $\varepsilon_i^{\text{OE}}$ the one-electron eigenenergy for the ith core state. Hence the CLS for the ith electron state in an A atom in an AB alloy calculated by using the Slater-Janak transition state [Eq. (8)] is

$$E_{\text{CLS}}^{\text{TS}(1,1/2)}(A_i) = \{E_F^{\text{alloy}}(1/2) - \varepsilon_i^{\text{OE,alloy}}(1/2)\},$$

$$- \{E_F^{\text{pure}}(1/2) - \varepsilon_i^{\text{OE,pure}}(1/2)\}. \qquad (10)$$

This method for calculating the CLS will be denoted "TS(1,1/2)."

In order to test the abovementioned assumption of linearity (Sec. II A) one may also calculate the TS-CLS by using Eq. (9):

$$E_{\text{CLS}}^{\text{TS}(1,0)}(A_i) = \{[E_F^{\text{alloy}}(1) - \varepsilon_i^{\text{OE,alloy}}(1)] + [E_F^{\text{alloy}}(0)$$

$$- \varepsilon_i^{\text{OE,alloy}}(0)]\} - \{[E_F^{\text{pure}}(1) - \varepsilon_i^{\text{OE,pure}}(1)]$$

$$+ [E_F^{\text{pure}}(0) - \varepsilon_i^{\text{OE,pure}}(0)]\}. \qquad (11)$$

The CLS calculated using this method will be denoted "TS(1,0)." The CLS calculated with these two methods will only be equal if the one-electron eigenenergy is a linear function of the occupation number. Apart from the transition-state model, the CLS can also be calculated by using the initial-state model[16] (IS) and the complete screening picture[13,17] (CS).

C. Computational details

1. Calculations

The metal systems calculated are Cu, Ag, Pd, Au, and Pt, for which the electronic states under investigation are $2p_{3/2}$, $3d_{5/2}$, $3d_{5/2}$, $4f_{7/2}$, and $4f_{7/2}$, respectively. For the alloys, only binary systems have been calculated, and these consists of different mixes of the metals above. For the pure Cu and Au systems, additional electronic states have also been calculated.

All computations were performed within the DFT using the Green's function technique based on the method according to Korringa, Kohn, and Rostocker (KKR) and the atomic sphere approximation (ASA).[4,18] The random alloy problem was solved within the coherent potential approximation[19,20] (CPA) and the cutoff for the basis set of linear muffin-tin orbitals[21,22] was set to $l_{max}=3$. For the exchange-correlation functional the generalized gradient approximation (GGA) according to Perdew *et al.*[23] was chosen. ASA+M (Refs. 24 and 25) is used throughout to account for multipole corrections to the ASA. Charge correlations were treated using the screened impurity model (SIM).[26–29] In the calculations theoretical equilibrium volumes are used. No local lattice relaxation effects due to size mismatch between alloy components are included. A complete description of the technique is given in Ref. 24.

The evaluation of the Kohn-Sham eigenvalues is performed numerically by adjusting the occupancy for the electron-state of interest. In order to maintain charge neutrality, the same amount that is removed from the core state is added to the valence band. The concentration of atoms for which the occupancy is varied is 1%.

2. Linearity

If the Kohn-Sham eigenvalues are *linear* functions of the occupation number η, they can be written as

$$\varepsilon(\eta) = \alpha \cdot \eta + \beta. \tag{12}$$

By comparing with Eq. (9) we see that in Eq. (12), α, which is the slope of the curve, corresponds to two times the final-state contribution to the binding energy and β corresponds to the initial-state contribution.

In order to investigate the linearity, the Kohn-Sham eigenvalues are calculated for occupation number η ranging from 0 to 1 in steps of 0.1, and the resulting eigenvalues are plotted as functions of η. This is done for several concentrations in the investigated alloys. The points are then used to perform linear interpolations of ε. For comparison, two simple estimates of the function are also performed, using two points only; one using $\eta=(1,1/2)$ and one using $\eta=(1,0)$. This corresponds to using Eq. (8) and (9) for calculating the binding energy, respectively. As mentioned in Sec. II B, these last two-point interpolations will only yield the same slope of the curve if the Kohn-Sham eigenvalues are linear functions of η.

Also, as a measure of the deviation from linearity, the norm of residuals is calculated:
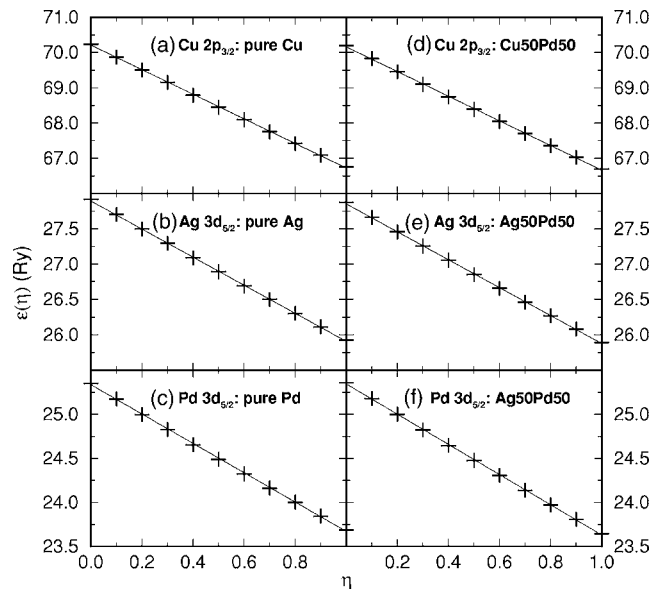

FIG. 1. Kohn-Sham eigenvalues for different systems as function of occupation number η. The lines in each graph have been taken from the linear interpolations and are shown as a guide to the eye.

$$\Delta = \frac{1}{n}\sqrt{\sum_{i=0}^{n}\{\varepsilon(x_i)^{\text{interpol}} - \varepsilon(x_i)^{\text{calc}}\}^2}, \tag{13}$$

where $x_i=(0,0.1,\dots,0.9,1.0)$, $\varepsilon^{\text{interpol}}$ are the linearly interpolated values and $\varepsilon^{\text{calc}}$ are the values from the first-principles calculations. However, since the norm of residuals depends on the magnitude of the eigenvalues, it is difficult to
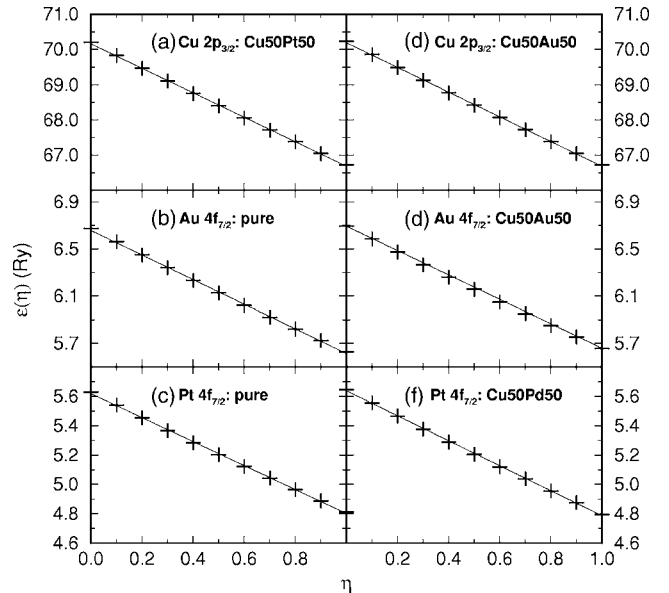

FIG. 2. Kohn-Sham eigenvalues for different systems as function of occupation number η. The lines in each graph have been taken from the linear interpolations and are shown as a guide to the eye.

TABLE I. Slopes of the function $\varepsilon(\eta) = \alpha \cdot \eta + \beta$ for different calculations. All slopes are in Ry. For the interpolated slope we used a linear interpolation for η ranging from 0 to 1 in steps of 0.1. The deviations D have been obtained by Eq. (14). See text for more details.

| System | Electron state | Slope (α) | | | Deviation |
		$\eta=(1,1/2)$	$\eta=(1,0)$	Interpolated	D
Cu	Cu $2p_{3/2}$	−3.39	−3.49	−3.48	0.016
Ag	Ag $3d_{5/2}$	−1.93	−1.99	−1.99	0.016
Pd	Pd $3d_{5/2}$	−1.61	−1.67	−1.66	0.023
Au	Au $4f_{7/2}$	−1.00	−1.05	−1.05	0.026
Pt	Pt $4f_{7/2}$	−0.78	−0.82	−0.82	0.027
$Ag_{50}Pd_{50}$	Pd $3d_{5/2}$	−1.66	−1.71	−1.71	0.019
$Ag_{50}Pd_{50}$	Ag $3d_{5/2}$	−1.92	−1.98	−1.98	0.018
$Cu_{50}Pd_{50}$	Cu $2p_{3/2}$	−3.38	−3.49	−3.49	0.018
$Cu_{70}Au_{30}$	Cu $2p_{3/2}$	−3.40	−3.50	−3.50	0.017
$Cu_{50}Au_{50}$		−3.40	−3.51	−3.51	0.018
$Cu_{30}Au_{70}$		−3.41	−3.52	−3.52	0.019
$Cu_{10}Au_{90}$		−3.41	−3.53	−3.53	0.020
$Cu_{90}Au_{10}$	Au $4f_{7/2}$	−1.00	−1.03	−1.03	0.022
$Cu_{70}Au_{30}$		−1.00	−1.04	−1.04	0.023
$Cu_{50}Au_{50}$		−1.00	−1.04	−1.04	0.024
$Cu_{30}Au_{70}$		−1.00	−1.04	−1.04	0.025
$Cu_{70}Pt_{30}$	Cu $2p_{3/2}$	−3.38	−3.48	−3.48	0.018
$Cu_{50}Pt_{50}$		−3.37	−3.48	−3.48	0.019
$Cu_{30}Pt_{70}$		−3.37	−3.48	−3.48	0.020
$Cu_{10}Pt_{90}$		−3.36	−3.49	−3.49	0.021
$Cu_{90}Pt_{10}$	Pt $4f_{7/2}$	−0.85	−0.88	−0.88	0.022
$Cu_{70}Pt_{30}$		−0.83	−0.87	−0.87	0.024
$Cu_{50}Pt_{50}$		−0.82	−0.85	−0.85	0.025
$Cu_{30}Pt_{70}$		−0.80	−0.84	−0.84	0.025

use Δ for comparing different electron-states. Therefore we define

$$D \equiv \frac{\Delta}{|\alpha|}, \qquad (14)$$

where α is the slope of the curve [Eq. (12)]. D will be used as a measure of the deviation from linearity.

The most accurate way to evaluate the binding energy integral, Eq. (7), is to perform numerical integration over the occupation numbers. The smaller the step is between two adjacent occupation numbers, the more accurate is the integral. For this numerical integration we have used the trapezoid rule[30] and varied the occupation number in steps of 0.1. This means totally 11 points are used for each binding energy, where each point correspond to one self-consistent calculation. For comparison, a numerical integration using the Simpson's rule[30] over three points (i.e., $\eta=0$, 1/2 and 1) has also been employed.

III. RESULTS AND DISCUSSION

A. The Kohn-Sham eigenvalues as a function of occupation numbers

The Kohn-Sham eigenvalues as function of the occupation numbers are shown for twelve different alloy systems in Figs. 1 and 2. We choose to present twelve graphs, though we have performed calculations on more systems (as can be seen in Tables I and II). From these two figures we see that, at least to a first approximation, the Kohn-Sham eigenvalues are linear functions of η. However, a more detailed analysis is needed before any conclusions may be drawn.

In Table I calculations of the slopes of the Kohn-Sham eigenvalues using different methods are presented. The first column show the alloy system, the next three show calculations of the slopes and the last one show the deviation from linearity, using Eq. (14).

We see that using the two points $\eta=(1,1/2)$ yields slopes that are less steep than those calculated using the two points $\eta=(1,0)$ or those from the linear interpolation. We also see

TABLE II. Slopes of the function $\varepsilon(\eta)=\alpha\cdot\eta+\beta$ for different electron-states in two metals, using different calculational methods. All slopes are in Ry. For the interpolated slope we used a linear interpolation for η ranging from 0 to 1 in steps of 0.1. The deviations D have been obtained by Eq. (14). See text for more details.

| System | Electron-state | Slope (α) | | | Deviation D |
		$\eta=(1,1/2)$	$\eta=(1,0)$	Interpolated	
Cu	Cu $2p_{1/2}$	−3.49	−3.59	−3.59	0.016
	Cu $2p_{3/2}$	−3.39	−3.49	−3.48	0.016
	Cu $3p_{3/2}$	−0.31	−0.37	−0.37	0.105
Au	Au $3d_{3/2}$	−4.69	−4.75	−4.75	0.007
	Au $3d_{5/2}$	−4.49	−4.55	−4.55	0.007
	Au $4s_{1/2}$	−1.29	−1.33	−1.33	0.018
	Au $4p_{1/2}$	−1.28	−1.32	−1.32	0.019
	Au $4d_{3/2}$	−1.13	−1.17	−1.17	0.021
	Au $4d_{5/2}$	−1.10	−1.14	−1.14	0.021
	Au $4f_{5/2}$	−1.02	−1.06	−1.06	0.026
	Au $4f_{7/2}$	−1.00	−1.05	−1.05	0.026

that the latter two methods are in better agreement with each other, as compared with the first one. This indicates that the eigenvalues are not perfectly linear functions, and show a slightly "concave" behavior.

From this table it is worth noting that for Cu $2p_{3/2}$ in CuAu and CuPt, D increases as the Cu concentration decrases. On the contrary, for Au $4f_{7/2}$ and Pt $4f_{7/2}$, D decrease as the concentration Au or Pt increase.

In Table II we present calculations similar to those in Table I, but carried out for several different electron-states in pure Cu and Au. From this table one may notice two interesting facts. First, the slope increases (i.e., the final-state contribution to the binding energy) the deeper into the atom the electron-state is located. This is expected, since the core-hole created when ejecting an electron will be more efficiently screened the deeper the level is, because there will be more electrons surrounding the hole. Secondly, the deviation (D) is somewhat smaller for deeper states than for those closer to the valence band.

B. Core level shifts

As mentioned in Sec. II B, the CLS as an application of Janak's theorem may show if devations from linearity of the Kohn-Sham eigenvalues has any noticable effect in physical observables. Figure 3 shows the CLS in CuAu for different transition-state calculations as a function of Au concentration. For the Cu $2p_{3/2}$ shift we see that there is a difference between the TS(1,1/2) and the TS(1,0) methods, and that it increases with the Au concentration. By comparing this observation with Table I, were we see that the deviation (D) from linearity increases with the Au concentration, it is clear that the difference between the two TS-CLS are due to the devation from linearity. For 90% Au, this difference is around 0.16 eV, which is rather large. One may also notice
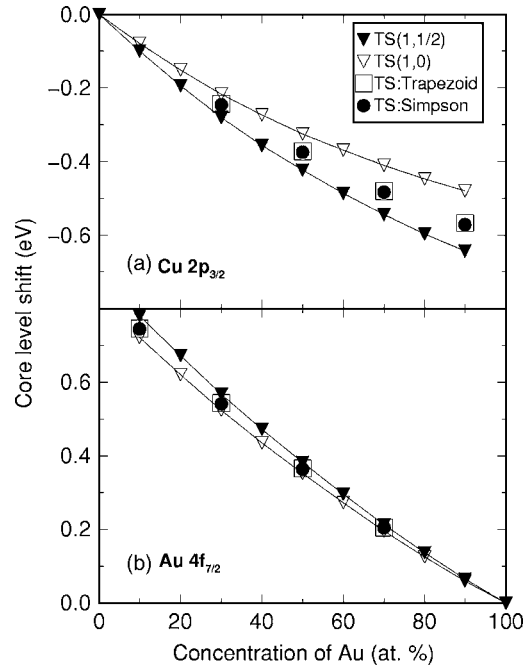

FIG. 3. CLS using different Transition State models for (a) Cu $2p_{3/2}$ and (b) Au $4f_{7/2}$ in CuAu as a function of the atomic concentration Au. Filled downward triangles ($\triangledown$) denote calculations using Eq. (11) (i.e., TS2), empty upward triangles ($\triangle$) denote calculations using Eq. (10) (i.e., TS1), empty squares ($\square$) denote numerical integration over all 11 occupation numbers, and filled circles ($\bullet$) denote numerical integration using Simpson's rule [i.e., over $\eta=(0,1/2,1)$].

that the shifts calculated using numerical integration over 11 and 3 points are very close to each other, and the results are in between the TS(1,1/2) and TS(1,0) shifts.

If we turn to the Au $4f_{7/2}$ shift we see that the TS(1,1/2) and the TS(1,0) CLS are closer to each other than the corresponding shifts in Cu $2p_{3/2}$. Table I indicates that the deviation (D) is larger for Au $4f_{7/2}$ than for Cu $2p_{3/2}$. However, the binding energy is much lower for the $4f_{7/2}$ level which causes the effect of the deviation from linearity to be smaller. Also here the shifts calculated using numerical integration over 11 and 3 points are close to each other, and in between the other two TS shifts.

In Fig. 4 the CLS in CuPt for different transition-state calculations is shown as a function of the concentration Pt. Starting with the Cu $2p_{3/2}$ shift, the situation is similar to that in Fig. 3. As for CuAu, Table I shows that Cu has an increasing deviation from linearity with increasing concentration Pt. Also, the difference between the TS(1,1/2) and the TS(1,0) methods increase with the concentration Pt. The largest difference between the TS(1,1/2) and TS(1,0) shifts is about 0.18 eV. The two shifts calculated by numerical integration are once again close to each other, but here they are closer to the TS(1,1/2) shift than to the TS(1,0) shift.

For the Pt $4f_{7/2}$ shift, the difference between the TS(1,1/2) and TS(1,0) shifts is very small, even though Table I indicates a relatively high deviation from linearity. This small difference is due to a small binding energy
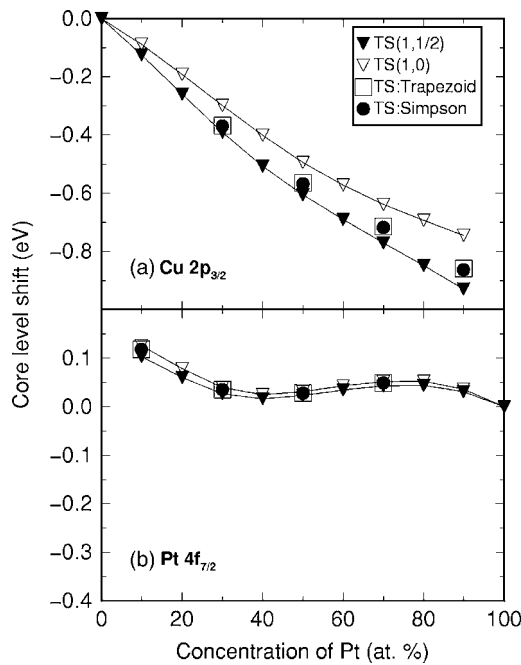
FIG. 4. CLS using different Transition State models for (a) Cu $2p_{3/2}$ and (b) Pt $4f_{7/2}$ in CuPt as a function of the atomic concentration Pt. Filled downward triangles (∇) denote calculations using Eq. (11) (i.e., TS2), empty upward triangles ($\triangle$) denote calculations using Eq. (10) (i.e., TS1), empty squares ($\square$) denote numerical integration over all 11 occupation numbers and filled circles ($\bullet$) denote numerical integration using Simpson's rule [i.e., over $\eta = (0, 1/2, 1)$].

FIG. 6. CLS for (a) Cu $2p_{3/2}$ and (b) Pt $4f_{7/2}$ in CuPt as a function of the atomic concentration Pt, using different methods. Filled circles ($\bullet$) denote numerical integration using Simpson's rule [i.e., over $\eta = (0, 1/2, 1)$], diamonds ($\diamond$) IS calculations and crosses ($\times$) CS calculations. Filled rightward triangles ($\blacktriangleright$) denote experimental results from Ref. 33 and filled leftward triangles ($\blacktriangleleft$) experimental results from Ref. 34.
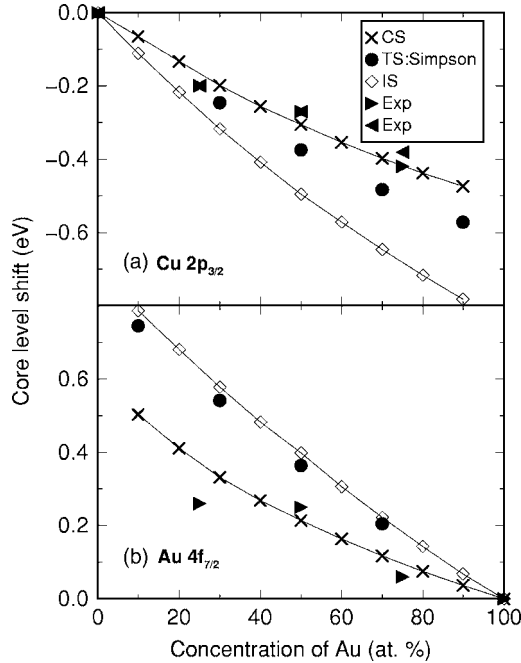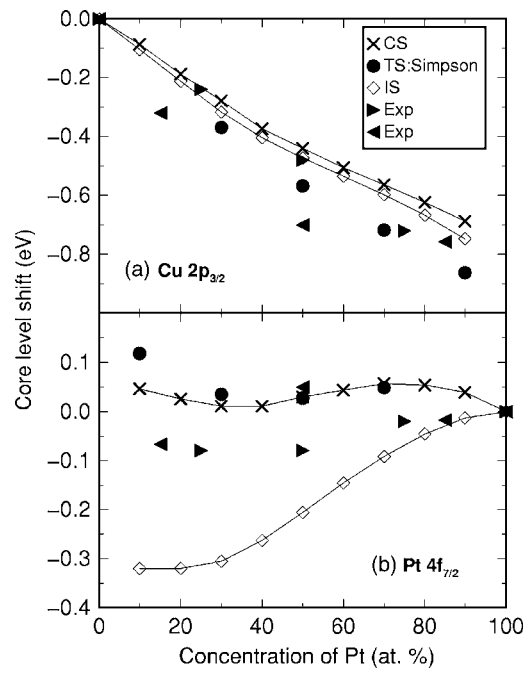

FIG. 5. CLS for (a) Cu $2p_{3/2}$ and (b) Au $4f_{7/2}$ in CuAu as a function of the atomic concentration Au, using different methods. Filled circles ($\bullet$) denote numerical integration using Simpson's rule [i.e., over $\eta = (0, 1/2, 1)$], diamonds ($\diamond$) IS calculations and crosses ($\times$) CS calculations. Filled rightward triangles ($\blacktriangleright$) denote experimental results from Ref. 31 and filled leftward triangles ($\blacktriangleleft$) experimental results from Ref. 32.

combined with a rather small CLS. The CLS from numerical integrations is in between the other two TS-CLS.

In order to compare our results for the Slater-Janak transition state model, we show the CLS in CuAu using different theoretical models and experimental results in Fig. 5. The TS-CLS shown in this figure employs numerical integration using the Simpson rule over $\eta = (0, 1/2, 1)$. For the Cu $2p_{3/2}$ shift we see that the CS-CLS is somewhat closer to the experimental values. Also, by comparing with the IS shift, one may notice that the CS-CLS has a larger final-state contribution than the TS-CLS has. Though there are differences, the agreement between the TS and CS shifts is reasonable.

The TS Au $4f_{7/2}$ shift is quite close to the IS shift. These two shifts are not very close to the CS shifts, which on the other hand is closer to the experimental results. The fact that the TS shift is close to the IS shift indicates that the TS model do not yield a large final-state contribution for Au $4f_{7/2}$ in CuAu. The reason for this difference is, to the best of our knowledge, not known.

Figure 6 shows the CLS in CuPt using the same methods as in Fig. 5. Starting with the Cu $2p_{3/2}$ shift, we see that the CS and IS shifts are quite close to each other, but the TS shift is not very far from these two. Since there is some discrepancy between the two different experimental shifts, it is difficult to conclude which one of the theoretical models that is closest to the experimental results. It may be worth noting that the TS shift has a negative final-state contribution, opposite to the Cu shift in CuAu.

The TS shift for Pt $4f_{7/2}$ is in good agreement with the CS shift, though the difference between the two increases with

decreasing Pt concentration. Also here, it is difficult to draw any conclusions about the agreement with experimental results, since there are differences between the different experimental shifts. The final-state contribution is quite large, both for the TS and CS shifts. The fact that the final-state contribution differs considerably between the TS and CS shifts for Au $4f_{7/2}$ but not for Pt $4f_{7/2}$ suggest that a more thourough study on the difference between the CS and TS models would be interesting.

IV. SUMMARY

We have performed ab-initio DFT calculations on 24 disordered alloy systems in order to verify if the Kohn-Sham eigenvalues are *linear* functions of the occupation number. To a first approximation, the eigenvalues show a linear dependence. However, for applications such as the calculation of core-level shifts, the deviation from linearity may have a noticeable effect.

The numerical integration using 11 values of the occupation numbers has been compared with the Simpson's rule integration over only 3 points ($\eta = 0, 1/2, 1$). Even for systems with considerable deviations from linearity, the difference between the two schemes for numerical integration is at most 0.7%, while the difference between either one of the traditional TS approaches [i.e., Eq. (8) or Eq. (9)] and the 11 point integration is up to 15%. This indicates that the three-point integration may be an alternative method to calculate the TS-CLS. It requires one more calculation than using TS(1,0) and two more than using TS(1,1/2), but should be more accurate.

[1] P. Hohenberg and W. Kohn, Phys. Rev. **136**, B864 (1964).

[2] W. Kohn and L. J. Sham, Phys. Rev. **140**, A1133 (1965).

[3] R. O. Jones and O. Gunnarsson, Rev. Mod. Phys. **61**, 689 (1989).

[4] J. S. Faulkner, Prog. Mater. Sci. **27**, 1 (1982).

[5] J. F. Janak, Phys. Rev. B **18**, 7165 (1978).

[6] M. M. Valiev and G. W. Fernando, Phys. Rev. B **52**, 10 697 (1995).

[7] M. Harris and P. Ballone, Chem. Phys. Lett. **303**, 420 (1999).

[8] F. W. Averill and G. S. Painter, Phys. Rev. B **46**, 2498 (1992).

[9] M. Methfessel, V. Fiorentini, and S. Oppo, Phys. Rev. B **61**, 5229 (2000).

[10] M. V. Ganduglia-Pirovano, M. Scheffler, A. Baraldi, S. Lizzit, G. Comelli, G. Paolucci, and R. Rosei, Phys. Rev. B **63**, 205415 (2001).

[11] W. Olovsson, C. Göransson, L. V. Pourovskii, B. Johansson, and I. A. Abrikosov, Phys. Rev. B **72**, 064203 (2005).

[12] J. C. Slater, *Quantum Theory of Molecules and Solids*, Vol. 4 of *International Series in Pure and Applied Physics*, 1st ed. (McGraw-Hill, New York, 1974).

[13] I. A. Abrikosov, W. Olovsson, and B. Johansson, Phys. Rev. Lett. **87**, 176403 (2001).

[14] W. R. L. Lambrecht, B. Segall, and O. K. Andersen, Phys. Rev. B **41**, 2813 (1990).

[15] N. Mårtenson, P. Hedegård, and B. Johansson, Phys. Scr. **29**, 154 (1984).

[16] W. F. Egelhoff, Jr., Surf. Sci. Rep. **6**, 253 (1987).

[17] B. Johansson and N. Mårtensson, Phys. Rev. B **21**, 4427 (1980).

[18] N. Papanikolaou, R. Zeller, and P. H. Dederichs, J. Phys.: Condens. Matter **14**, 2799 (2002).

[19] P. Soven, Phys. Rev. **156**, 809 (1967).

[20] B. Velicky, S. Kirkpatrick, and H. Ehrenreich, Phys. Rev. **175**, 747 (1968).

[21] O. K. Andersen and O. Jepsen, Phys. Rev. Lett. **53**, 2571 (1984).

[22] O. K. Andersen, Phys. Rev. B **12**, 3060 (1975).

[23] J. P. Perdew, K. Burke, and M. Ernzerhof, Phys. Rev. Lett. **77**, 3865 (1996).

[24] I. A. Abrikosov and H. L. Skriver, Phys. Rev. B **47**, 16532 (1993); A. V. Ruban and H. L. Skriver, Comput. Mater. Sci. **15**, 119 (1999).

[25] P. A. Korzhavyi, I. A. Abrikosov, B. Johansson, A. V. Ruban, and H. L. Skriver, Phys. Rev. B **59**, 11 693 (1999).

[26] P. A. Korzhavyi, A. V. Ruban, I. A. Abrikosov, and H. L. Skriver, Phys. Rev. B **51**, 5773 (1995).

[27] A. V. Ruban, I. A. Abrikosov, and H. L. Skriver, Phys. Rev. B **51**, 12 958 (1995).

[28] A. V. Ruban and H. L. Skriver, Phys. Rev. B **66**, 024201 (2002).

[29] A. V. Ruban, S. I. Simak, P. A. Korzhavyi, and H. L. Skriver, Phys. Rev. B **66**, 024202 (2002).

[30] L. Råde and B. Westergren, *Mathematics Handbook*, 3rd ed. (Studentlitteratur, Lund, 1998).

[31] M. Kuhn and T. K. Sham, Phys. Rev. B **49**, 1647 (1994).

[32] T. K. Sham, A. Hiraya, and M. Watanabe, Phys. Rev. B **55**, 7585 (1997).

[33] A. W. Newton, S. Haines, P. Weightman, and R. J. Cole, J. Electron Spectrosc. Relat. Phenom. **136**, 235 (2004); A. W. Newton, Ph.D. thesis, University of Liverpool, Liverpool, 2001.

[34] Y.-S. Lee, K.-Y. Lim, Y.-D. Chung, C.-N. Whang, and Y. Jeon, Surf. Interface Anal. **30**, 475 (2000).